2009 International Symposium on Nonlinear Theory and its Applications
NOLTA'09, Sapporo, Japan, October 18-21, 2009

Basic Coding Functions of Paralleled Chaotic Spiking Neurons

Hiroyuki Torikai† and Toru Nishigami†

†Graduate School of Engineering Science, Osaka University, 1-3 Machikaneyama-cho,
Toyonaka, Osaka 560-8531, Japan. Email: torikai@sys.es.osaka-u.ac.jp

Abstract—In this paper we investigate an artificial spiking neuron model inspired by the mammalian spiral ganglion cell. It is shown, by numerical analysis and SPICE simulations, that a set of paralleled N neurons can encode an analog input signal in such a way that (1) a spike histogram of summation of the N spike-trains can mimic waveform of the analog input, (2) the spike-trains do not synchronize to each other and thus the summed spike-train can have higher sampling rate, and (3) firing rates of the neurons can be adjusted by internal parameters.

1. Introduction

Fig.1 shows a sketch of the mammalian inner ear [1]. The spiral ganglion cell encodes a periodic sinusoidal input $P(t)$ (which is a receptor potential of the inner hair cell) into a spike-train $Y_i(t)$. Physiological experiments show that a set of paralleled N spiral ganglion cells encodes the periodic input $P(t)$ into the summed spike-train $Y(t) = \sum_i Y_i(t)$ in such a way that a spike histogram of the summed spike-train $Y(t)$ mimics the waveform of the input $P(t)$, where $N \simeq 20$ in the case of humans. In this paper such an encoding function of paralleled spiking neurons is referred to as a *paralleled spike encoding function*.

Inspired by this encoding function, in this paper we investigate an artificial *chaotic spiking neuron* (CSN) as sketched in Fig.2(a). The CSNs accept the input $s(\tau)$ which can have various waveforms such as constant, periodic, non-periodic and random waveforms. It is shown, by numerical analysis and SPICE simulations, that a set of N CSNs can realize a paralleled spike encoding function which utilizes the following properties: (P1) a spike histogram of the summed spike-train $y(\tau) = \sum_{i=1}^{N} y_i(\tau)$ mimics waveform of the input $s(\tau)$; (P2) the spike-trains $\{y_1(\tau), \cdots, y_N(\tau)\}$ do not synchronize to each other and thus the summed spike-train $y(\tau)$ can have N times higher encoding resolution than each single spike-train $y_i(\tau)$; and (P3) firing rates of the CSNs are adjustable and thus operation speeds of chip-implemented CSNs are adjustable.

Significances of this paper are including the following points: (i) Synthesis of an artificial spiking neuron model and analysis of its encoding function are important fundamental researches to develop pulse-coupled neural networks and their applications [2]-[8]. (ii) The paralleled spike encoding function can be applied to paralleled analog-to-digital converters, where $s(\tau)$ is an analog input and $\{y_1(\tau), \cdots, y_N(\tau)\} \in \{0, 1\}^N$ are paralleled digital outputs. It has been pointed out that such spike-timing-based analog-to-digital converters are promising in a future VLSI technology because it will become more difficult to obtain an analog circuit having high precision of state variables (e.g., capacitor voltage) as the integration size decreases [5][9]. (iii) Since the CSN is a generalized system of the artificial spiral ganglion cell model in [7], it may contribute to develop a future biologically plausible cochlea implant [1][10]. Such a biologically plausible cochlea implant should include a huge number of artificial spiral ganglion cells like the mammalian inner ear. The presented CSN is suitable for this purpose since it can be implemented by a simple circuit.

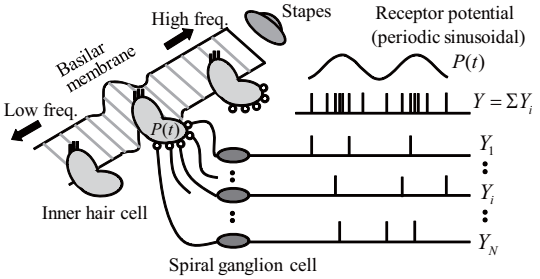

Figure 1: Basic mechanisms of the mammalian inner ear [1]. A spike histogram of the summed spike-train $Y(t) = \sum_i Y_i(t)$ of the spiral ganglion cells mimics waveform of a periodic sinusoidal receptor potential $P(t)$ of the inner hair cell.

2. Paralleled chaotic spiking neurons

In this section we investigate a mathematical model of the paralleled *chaotic spiking neurons* (CSNs) whose block diagram is shown in Fig.2(a). As show in this figure each CSN consists of two units: the *base unit* which is commonly used by all the CSNs and the *neuron unit* which is individually used by each CSN. The input $s(\tau)$ is commonly applied to the base unit and the neuron units. Fig.2(b) shows an example of the input $s(\tau)$, where $\tau \geq 0$ is a dimensionless time. In this paper we assume that the input $s(\tau)$ can have various waveforms (e.g., constant, periodic, non-periodic, and random) under the following condition for all $\tau \geq 0$.

$$\begin{array}{l} \int s(\tau)\, d\tau \ \text{ is continuous, and there exists} \\ \text{a constant } s_{max} < \infty \text{ such that } \ |s(\tau)| \leq s_{max}. \end{array} \quad (1)$$

This condition says that the input $s(\tau)$ should be bounded and should not include the Dirac's delta function. Most

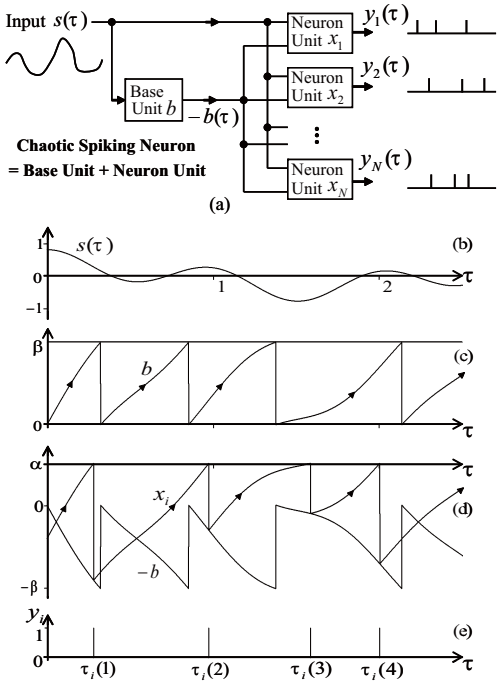

Figure 2: Chaotic spiking neuron (CSN) and its basic dynamics. (a) The CSN consists of the base unit and the neuron unit. (b) As an example of the input $s(\tau)$, a non-periodic input $s(\tau)$ is shown. (c) Integrate-and-fire-type dynamics of the state b of the base unit. (d) Integrate-and-fire-type dynamics of the state x_i of the neuron unit. At the firing moment, the state x_i is reset to the base signal $-b$. (e) Output spike-train $y_i(\tau)$.

of realistic inputs $s(\tau)$ satisfy this condition. As shown in Fig.2(a) the base unit has an internal state b. Fig.2(c) shows basic dynamics of the state b that is described by the following integrate-and-fire-type equation.

$$\begin{cases} \dot{b} = s(\tau) + s_0 & \text{for } b(\tau) < \beta, \\ b(\tau^+) = 0 & \text{if } b(\tau) = \beta \end{cases} \tag{2}$$

where $\dot{b}$ represents $db/d\tau$, τ^+ represents $\lim_{\epsilon\to 0}\tau+\epsilon$, $\epsilon > 0$, and the initial state $b(0)$ is assumed to satisfy $b(0) \le \beta$. We refer to the parameters s_0 and β as a *stimulation offset* and a *firing threshold*, respectively. The parameters (s_0, β) are assumed to satisfy the following condition.

$$s(\tau) + s_0 > 0, \quad \beta > 0. \tag{3}$$

As shown in Fig.2(c) the state b increases by integrating the positive signal $s(\tau) + s_0$. If the state b reaches the firing threshold β at τ, the state b is reset to zero at τ^+. Repeating such integrate-and-fire dynamics, the state b oscillates. As shown in Fig.2(a) the signal $-b(\tau)$ is used as an output of the base unit. Hence we refer to $-b(\tau)$ as a *base signal*. The base signal $-b(\tau)$ is commonly input to the N neuron units. As shown in Fig.2(a) each i-th neuron unit has an internal state x_i and an output y_i. Fig.2(d) and (e) show basic dynamics of the state x_i and the output y_i that are described by the following integrate-and-fire-type equation.

$$\begin{cases} \dot{x}_i = s(\tau) + s_0 & \text{for } x_i(\tau) < \alpha, \\ x_i(\tau^+) = -b(\tau^+) & \text{if } x_i(\tau) = \alpha, \end{cases}$$
$$y_i(\tau) = \begin{cases} 0 & \text{for } x_i(\tau) < \alpha, \\ 1 & \text{if } x_i(\tau) = \alpha, \end{cases} \tag{4}$$

where $i = 1, 2, \cdots, N$. The parameter α is referred to as a *firing threshold* and is assumed to satisfy

$$\alpha > 0. \tag{5}$$

The neuron units are assumed to have different initial states $x_i(0) \neq x_j(0)$, $x_i(0) \le \alpha$, $x_j(0) \le \alpha$ for all $i \neq j$. As shown in Fig.2(d), the state x_i increases by integrating the positive signal $s(\tau) + s_0$. If the state x_i reaches the firing threshold α at τ, the state x_i is reset to the base signal $-b(\tau)$ at τ^+. At this reset moment, the i-th neuron unit outputs a firing spike $y_i(\tau) = 1$ as shown in Fig.2(e). Repeating such integrate-and-fire dynamics, the i-th neuron unit outputs a spike-train $y_i(\tau)$ as shown in Fig.2(e). As shown in Fig.2(a) the spike-trains $\{y_1, \cdots, y_N\}$ are summed:

$$y(\tau) = \sum_{i=1}^{N} y_i(\tau). \tag{6}$$

We can summarize the system description as the following: the input $s(\tau)$ can have arbitrary waveform under the condition in Equation (1); the CSNs are described by Equations (2) and (4); the CSNs are characterized by the parameters (N, s_0, β, α) satisfying the conditions in Equations (3) and (5); and the spike-trains of the CSNs are summed as described in Equation (6).

3. Numerical simulations and Paralleled encoding

In this section we investigate whether the paralleled CSNs satisfy the properties (P1), (P2) and (P3), and investigate how the input $s(\tau)$ is encoded into the summed spike-train $y(\tau)$. Let us begin with defining a *spike histogram* and a *firing rate*. The *spike histogram* $\tilde{\rho}(\tau)$ of the summed spike-train $y(\tau) = \sum_{i=1}^{N} y_i(\tau)$ is defined by

$$\tilde{\rho}(\tau) \equiv \frac{\#\text{ of spikes in } y(\tau) \text{ for } m\delta \le \tau < (m+1)\delta}{N\delta} \tag{7}$$

where $\delta > 0$ is the histogram bin size, $m = 0, 1, 2, \cdots$, and "$\equiv$" denotes the "definition" hereafter. The *firing rate* γ_i of a single spike-train $y_i(\tau)$ is defined by

$$\gamma_i \equiv \lim_{T\to\infty} \frac{\#\text{ of spikes in } y_i(\tau) \text{ for } 0 \le \tau < T}{T}. \tag{8}$$

Fig.3 shows numerical simulation results (by the trapezoidal numerical integration) for some typical inputs $s(\tau)$, where the parameters are fixed to

$$N = 20, \quad s_0 = 1, \quad \beta = 0.5, \quad \alpha = 0.5\beta. \tag{9}$$

We can see in Fig.3 that the input $s(\tau)$ is encoded into the summed spike-train $y(\tau)$ as the followings.

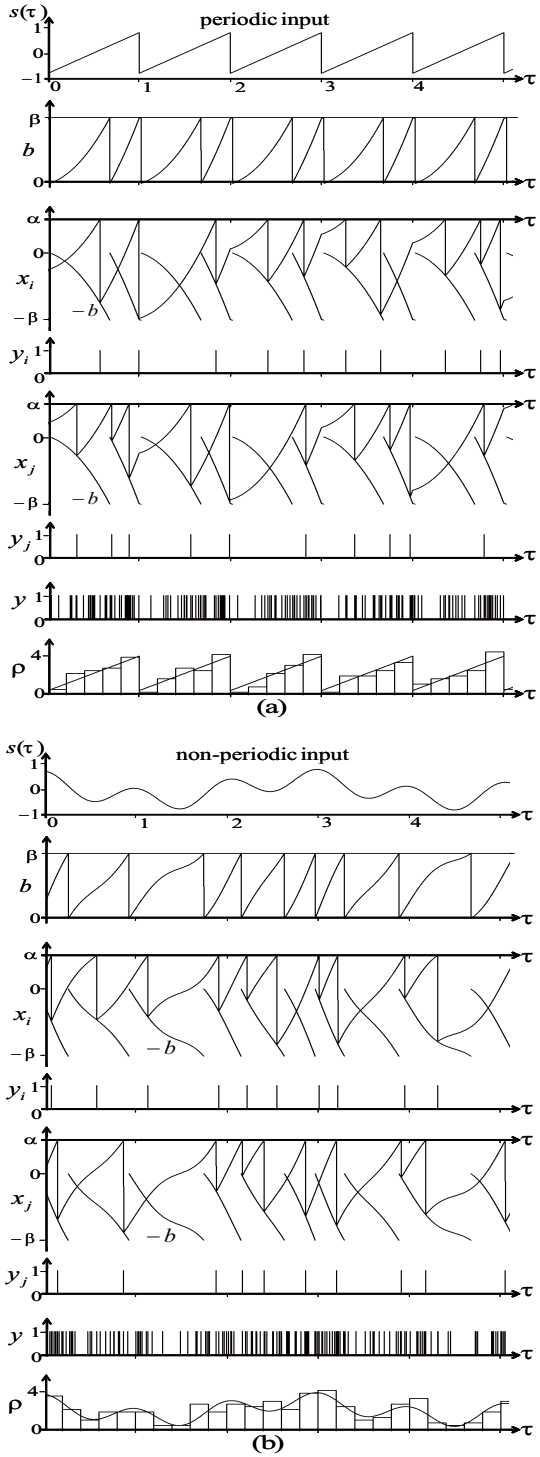

Figure 3: Paralleled spike encoding function of the CSNs. The parameters (N, β, α, s_0) are fixed to $(20, 0.5, 0.25, 1)$. $y(\tau) = \sum_{i=1}^{20} y_i(\tau)$ is the summation of $N = 20$ spike-trains. $\tilde{\rho}(\tau)$ is the spike histogram of the summed spike-train $y(\tau)$ defined in Equation (7). (a) Periodic sawtooth input $s(\tau)$ in Equation (10). (b) Non-periodic input $s(\tau)$ described in Equation (13). In both (a) and (b), the firing rates are $(\gamma_i, \gamma_j) \simeq (2, 2)$, the spike histogram $\tilde{\rho}(\tau)$ (rectangles) mimics the waveforms of scaled inputs $2(s(\tau) + 1)$ (solid lines and curve), and the spike-trains (y_i, y_j) do not synchronize.

3.1. Periodic input

In the case of Fig.3(a), the input $s(\tau)$ is give by the following periodic sawtooth signal

$$\begin{aligned} &s(\tau) = 1.6(\tau - 0.5) \quad \text{for } 0 \le \tau < 1, \\ &s(\tau + 1) = s(\tau). \end{aligned} \tag{10}$$

It can be seen in Fig.3(a) that the states $\{x_i, x_j\}$ of the CSNs do synchronize and the corresponding spike-trains $\{y_i, y_j\}$ do not synchronize. We have also confirmed (but not shown in the figure) that the spike-trains $\{y_1, \cdots, y_N\}$ of all the CSNs do not synchronize. Hence the CSNs satisfy the property (P2). In Fig.3(a) the summed spike-train $y(\tau) = \sum_{i=1}^{20} y_i(\tau)$ and its spike histogram $\tilde{\rho}(\tau)$ are also shown. We can see the following relation between the input $s(\tau)$ and the spike histogram $\tilde{\rho}(\tau)$.

$$\tilde{\rho}(\tau) \simeq 2(s(\tau) + 1). \tag{11}$$

This equation means that the spike histogram $\tilde{\rho}(\tau)$ mimics the waveform of the input $s(\tau)$ and thus the CSNs satisfy the property (P1). In the case of Fig.3(a) the firing rates γ_i and γ_j of the spike-trains y_i and y_j are given by

$$\gamma_i \simeq 2, \quad \gamma_j \simeq 2. \tag{12}$$

We have also confirmed (but not shown in the figure) that all the firing rates $\{\gamma_1, \cdots, \gamma_N\}$ are approximately two.

3.2. Non-periodic input

In the case of Fig.3(b), the input $s(\tau)$ is

$$s(\tau) = 0.4\cos(2\pi\tau) + 0.4\cos\left(\frac{2\pi}{\sqrt{10}}\tau\right). \tag{13}$$

This input $s(\tau)$ is non-periodic. It can be seen in Fig.3(b) that the spike-trains $\{y_i, y_j\}$ of the CSNs do not synchronize. We have also confirmed (but not shown in the figure) that the spike-trains $\{y_1, \cdots, y_N\}$ of all the CSNs do not synchronize. Hence the CSNs satisfy the property (P2). In Fig.3(b) we can see the following relation between the input $s(\tau)$ and the spike histogram $\tilde{\rho}(\tau)$.

$$\tilde{\rho}(\tau) \simeq 2(s(\tau) + 1). \tag{14}$$

This equation means that the spike histogram $\tilde{\rho}(\tau)$ mimics the waveform of the input $s(\tau)$ and thus the CSNs satisfy the property (P1). In the case of Fig.3(b) the firing rates are given by

$$\gamma_i \simeq 2, \quad \gamma_j \simeq 2. \tag{15}$$

We have also confirmed (but not shown in the figure) that all the firing rates $\{\gamma_1, \cdots, \gamma_N\}$ are approximately two.

3.3. Paralleled encoding function

From the above numerical simulation results, we can provide a hypothesis that the input $s(\tau)$ is encoded into the spike histogram $\tilde{\rho}(\tau)$ as

$$\tilde{\rho}(\tau) \simeq (s(\tau) + s_0)/\beta$$

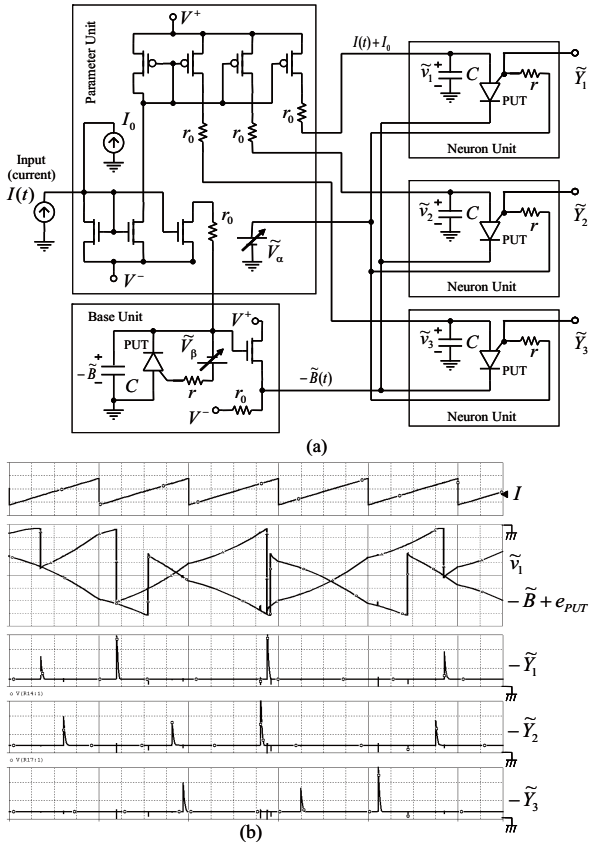

Figure 4: Transistor model of the paralleled CSNs. (a) Whole circuit structure for $N = 3$ CSNs. The input $I(t)$ is given as a current signal. (b) SPICE simulation result. Horizontal axis is 0.5μsec/div.. Vertical axes are I : 1mA/div., $(-\tilde{B} + e_{PUT}, v_i)$: 1V/div. and $-\tilde{Y}_i$: 2V/div.. The black triangle indicates $I = 0$. $I_0 = 1.8$[mA], $r_0 = 1[\Omega]$, $r = 5[\Omega]$, $V^+ = 10$[V], $V^- = -10$[V], $C = 10$[nF], $\tilde{V}_\beta = 5$[V], $\tilde{V}_\alpha = -1$[V]. As the PUT, a SPICE model of the discrete circuit element 2N6027 is used. The SPICE parameters of the pMOS transistors are: $L = 10^{-6}$, $W = 10^{-5}$ and the other parameters are the same as the discrete circuit element M2SJ325. The SPICE parameters of the nMOS transistors except for the one in the base unit are: $L = 10^{-6}$, $W = 10^{-5}$ and the other parameters are the same as the discrete circuit element 2SK1580. The SPICE parameters of the nMOS transistor in the base unit are the same as that of the discrete circuit element 2SK1850.

and thus the CSNs satisfy the property (P1). We can also provide a hypothesis that the spike-trains $\{y_1, \cdots, y_N\}$ do not synchronize and the CSNs satisfy the property (P2). In addition we can provide a hypothesis that the firing rate γ_i of each spike-train y_i is given by

$$\gamma_i = s_0/\beta$$

and thus the CSNs satisfy the property (P3). These hypotheses are theoretically true as proven in [8].

We present a transistor model of the paralleled CSNs in Fig.4(a). Using appropriate transformations, the circuit equation is transformed into Equations (2) and (4). Fig.4(b) shows a SPICE simulation result. It can be seen that more spikes are generated as the input $I(t)$ has a larger value and that the spike-trains $\{-\tilde{Y}_1, -\tilde{Y}_2, -\tilde{Y}_3\}$ do not synchronize. Hence the transistor model satisfies the properties (P1) and (P2). We have also confirmed (but not shown by pictures) that the transistor model satisfies the property (P3).

4. Conclusions

We have analyzed the paralleled spike encoding function (which utilizes the properties (P1), (P2) and (P3)) of the chaotic spiking neuron. Also we have presented the electronic circuit model of the neuron and confirmed the typical paralleled encoding function by SPICE simulations. Future problems include the followings: (a) analysis of robustness of the encoding function against parameter mismatches; (b) design of the CSN for VLSI implementation; and (c) analysis of the encoding function from AD converter viewpoints, e.g., limitation of sampling rate, signal-to-noise ratio, noise shaping, power consumption and implementation size.

The authors would like to thank Professor Toshimitsu Ushio of Osaka University for valuable discussions. This work is partially supported by the Center of Excellence for Founding Ambient Information Society Infrastructure, Osaka University, Japan; the Grant-in-Aid for Young Scientists (KAKENHI); and TAF.

References

[1] Geisler, C. D. (1998). From sound to synapse: physiology of the mammalian ear, Oxford University Press.

[2] Izhikevich, E.M. (2006). Dynamical systems in neuroscience, MIT Press.

[3] Gerstner, W. and Kistler, W (2002). Spiking neuron models, Cambridge University Press.

[4] Eckhorn, R. (1999). Neural mechanisms of scene segmentation: recordings from the visual cortex suggest basic circuits for linking field models, IEEE Trans. Neural Networks, vol.10, no.3, pp.464-479.

[5] Hamanaka, H., Torikai, H., and Saito, T. (2006). Quantized spiking neuron with A/D conversion functions, IEEE Trans. CAS-II, vol. 53, no. 10, pp. 1049-1053.

[6] Torikai, H., Funew, A., and Saito, T. (2008). Digital spiking neuron and its learning for approximation of various spike-trains, Neural Networks, 21, 2-3, pp. 140-149.

[7] Torikai, H., and Nishigami, T. (2008). A novel artificial model of spiral ganglion cell and its spike-based encoding function, Proc. of ICONIP2008. (to appear).

[8] Torikai, H., and Nishigami, T. (2009). An artificial chaotic spiking neuron inspired by spiral ganglion cell: paralleled spike encoding, theoretical analysis, and electronic circuit implementation, Neural Networks (in press).

[9] Wei, D. and Harris, J. (2004). Signal reconstruction from spiking neuron models, Proc. of IEEE/ISCAS, vol.V, pp.353-356.

[10] Martignoli, S., van der Vyver, J.-J., Kern, A., Uwate, Y., and Stoop, R. (2007). Analog electronic cochlea with mammalian hearing characteristics, Applied Physics Letters, 91, 064108.